Mathematical Biosciences and Engineering

https://www.aimspress.com/journal/mbe

MBE, 23(7): 1971–1994.
DOI: 10.3934/mbe.2026072
Received: 15 February 2026
Revised: 30 April 2026
Accepted: 01 June 2026
Published: 02 July 2026

Research article

Dynamic analysis of a SEAIRS model on co-evolution of human behavior changes in COVID-19 epidemic

Xiaoyu Li[1], Nan Wang[1] and Zhiming Li[2,*]

[1] Basic Teaching Department, Xinjiang University of Political Science and Law, Tumushuke 843900, China

[2] College of Mathematics and System Science, Xinjiang University, Urumqi 830017, China

* **Correspondence:** Email:zmli@xju.edu.cn.

Abstract: Considering that people usually take non-drug protective measures (making behavior changes), this paper proposes a new SEAIRS model by combining behavior changes during the spread of the COVID-19 epidemic. First, we prove the positivity and boundedness of the solution of the model. Furthermore, the existence and stability of the equilibrium points are discussed in three behavior scenarios ($B_c = 0$, $B_c = 1$, $0 < B_c < 1$, where B_c represents the proportion of susceptible individuals (S), exposed individuals (E), and asymptomatic infected individuals (A) who adopt preventive behavior changes). Finally, we illustrate the model's behaviour using COVID-19 data from Romania, and summarize some valuable results: (i) the spread of diseases can be effectively controlled by reducing the contact between susceptible, exposed, and infected individuals; (ii) increasing the proportion of behavioral changes can significantly reduce the number of infected individuals. The model suggests two main theoretical measures to promote behavior changes within the framework: one is to increase the return difference between the two behaviors by adjusting relevant parameters, and the other is to increase the value of the information function.

Keywords: COVID-19 epidemic; SEAIRS model; behavior change; globally asymptotically stable

1. Introduction

The COVID-19 outbreak, which began at the end of 2019, is an infectious disease caused by the SARS CoV-2 virus. This virus has a strong transmission ability and high pathogenicity [1–3]. In the early stages of the outbreak, many scholars primarily focused on the basic transmission mechanism of the virus, thereby extending the classic SIR (Susceptibility, Infection, Recovery) model to various mathematical models such as SAIR and SEIR for research, prediction, prevention and control of the epidemic [4–10]. For example, Ansumali et al. [4] established a class of SAIR compartment

models that considered population migration based on the asymptomatic infection characteristics of COVID-19, and discussed the global asymptotic stability of equilibrium points using the Lyapunov theory. In addition, parameter estimation methods were proposed and applied to multi-country data prediction. Singh and Bajpai [5] proposed a new SEIHCRD model that can more accurately predict the spread, number of cases, mortality rate, and medical resource demand of COVID-19 by extending the SEIR model and adding three compartments: death, hospitalization, and critical illness. Ramos et al. [8] developed a simplified but sufficiently complex SIR model called theta SEIHQRD, which effectively simulates the transmission dynamics of COVID-19 in Italy and the impact of different prevention and control measures. The models in this stage mostly focus on the transmission characteristics of the virus itself, thereby emphasizing the transformation laws between different populations, thus laying the foundation for subsequent research on infectious disease dynamics models. However, the regulatory role of human behavior on epidemic transmission has not been fully considered.

In recent decades, behavioral dynamics in epidemic modeling have been widely studied. Poletti et al. [11, 12] pioneered game-theoretic frameworks, while Funk et al. [13] and Verelst et al. [14] provided systematic reviews. Jentsch et al. [15] further applied the evolutionary game theory to study vaccination behaviors. With the widespread outbreak of the COVID-19 pandemic in recent years, non-pharmacological interventions such as isolation, social distancing, and mask-wearing have been widely practiced worldwide. In response, scholars have gradually incorporated these behaviors into model frameworks to enhance the practical applicability and align with real-world scenarios [16–24]. For example, Mandal et al. [19] developed a SEQIR model with isolation and prevention measures to mitigate COVID-19 transmission and showed that both the quarantine and governmental intervention strategies, such as implementing blockades, strengthening media coverage on social distancing, and improving public hygiene, can reduce the spread of COVID-19. Zhang et al. [20] proposed a two-layer network SEIX model, thereby combining the transmission of infectious diseases with human isolation dynamics. The author's research results indicate that the spread of contagious diseases can be controlled when a certain proportion of individuals voluntarily isolate. Das et al. [22] analyzed an extended SEIR model and quantified the detection ratio required for isolation effectiveness. Arif et al. [24] constructed a SEIQR model with isolation, and validated its predictive accuracy via a theoretical analysis and MATLAB simulation, thus highlighting isolation's key role in epidemic control.

However, although the epidemic models mentioned above incorporate individual protective behaviors, they focus on only one or a few specific protective measures and fail to fully consider the diversity and dynamic evolution of individual behaviors in real-world scenarios. This limitation reduces their practical explanatory power and application value. In this regard, Tang et al. [25] developed a more comprehensive framework that uniformly addresses individuals' behavioral changes based on game-theoretic methods [26–29]. Their research systematically integrates behavioral changes with disease transmission, clarifying their impact on susceptibility and infectivity, which represents an important progress in behavioral modeling. In detail, they divided the total population (N) into susceptible (S), exposed (E), asymptomatic infected (A), symptomatic infected (I), diagnosed and isolated (H), symptomatic recovered (R_I) and asymptomatic recovered (R) individuals. The model is based on the following assumptions: (i) once the infected person is diagnosed, they will be immediately quarantined, and the quarantined person (H) cannot transmit the

virus; (ii) asymptomatic infected people will not transfer to symptomatic (I) and will eventually become recovered, and (iii) individuals without symptoms (S, E, A, R) can reduce their susceptibility or contagiousness by changing their behavior. Under the above assumptions, (S, E, A, R) are partitioned into two subcategories, namely, individuals who do not change their behavior (S_n, E_n, A_n, R_n) and individuals who change their behavior (S_c, E_c, A_c, R_c). Through ordinary differential equations, the disease transmission model is established as follows:

$$\begin{cases} S_n'(t) = -\lambda S_n, \\ S_c'(t) = -q\lambda S_c, \\ E_n'(t) = \lambda S_n - \sigma E_n, \\ E_c'(t) = q\lambda S_c - \sigma E_c, \\ A_n'(t) = (1-\varrho)\sigma E_n - \gamma_A A_n, \\ A_c'(t) = (1-\varrho)\sigma E_c - \gamma_A A_c, \\ I'(t) = \varrho\sigma E_n + \varrho\sigma E_c - (\delta_I(t) + \gamma_I)\, I, \\ H'(t) = \delta_I(t) I - (\alpha(t) + \gamma_H)\, H, \\ R_I'(t) = \gamma_I I + \gamma_H H, \\ R_n'(t) = \gamma_A A_n, \\ R_c'(t) = \gamma_A A_c, \end{cases} \tag{1.1}$$

where $\lambda = (\beta_I I + \beta_A A_n + q\beta_A A_c)/N$ is the force of infection, and the notations β_I and β_A are the effective propagation coefficients of I and A, respectively. The parameter q ($0 \le q \le 1$) is the proportion of the decrease in propagation rate caused by the changing behavior, $1/\sigma$ represents the incubation period, and $\delta_I(t)$ denotes the time-varying diagnostic rate. The proportion of σE transferred to I is recorded as ϱ, $\alpha(t)$ is the mortality rate caused by diseases, and $(\gamma_I, \gamma_A, \gamma_H)$ are the recovery rates of (I, A, H), respectively. Next, they used an information index to describe the phenomenon of infection risk promoting the evolution of human behavior, and set its form as follows:

$$M'(t) = a\delta_I(t) I - \eta M,$$

where a measures the level of acceptance of information obtained from confirmed cases $\delta_I(t)I$, and η is the decay rate of the information index. Tang et al.'s model is an early attempt to capture the interaction between human behavioral changes and COVID-19 transmission dynamics using the evolutionary game theory. Due to its pioneering nature, it serves as the baseline framework for our study.

In practice, Model (1.1) has several limitations: (i) as a potential source of infection, the exposed individuals E pose a risk of disease transmission, thus, λ is lower than the actual infectivity of the disease; (ii) some asymptomatic infected individuals directly transfer to recovered individuals after some time, while others transfer to the symptomatic infected; and (iii) the individuals in H are isolated and do not promote the spread of the virus so that we can ignore them. Given the above, the innovation of this paper mainly includes several aspects: we first establish a novel SEAIRS model to make up the shortcomings (i)–(iii) of Tang et al.'s model, thereby revealing the impact of behavioral changes on disease transmission; then, the existence and stability of disease-free and endemic equilibria of the model are obtained based on different behavior changes; and finally, we illustrate the model's behaviour using real data. The rest of this paper is organized as follows: in Section 2, a new SEAIRS model with behavioral changes is presented; in Section 3, the dynamic properties of the SEAIRS system

are obtained, including the positivity and boundedness of the solution, as well as the stability of all equilibrium points; in Section 4, we conduct several numerical simulations and parameter analyses to validate the theoretical results; in Section 5, we illustrate the model's behaviour using COVID-19 data from Romania and discuss it accordingly; and a brief conclusion is given in Section 6. The main contributions of this paper are as follows: (i) extending existing behavioral models to include the infectivity of exposed individuals and the asymptomatic-to-symptomatic transition; (ii) introducing a saturated information index that better reflects real-world information propagation; (iii) providing a rigorous theoretical analysis of the coupled system; and (iv) illustrating the model's behaviour with real data.

2. A SEAIRS model with behavior changes

Suppose the total population $N(t)$ is divided into susceptible, exposed, asymptomatic infected, symptomatic infected, and recovered individuals at time t. Let $S(t), E(t), A(t), I(t)$, and $R(t)$ be the corresponding proportions at time t. Among them, S, E, and A are further classified as two groups based on whether they change their behavior, namely individuals who do not change their behavior (S_n, E_n, A_n) and individuals who change their behavior (S_c, E_c, A_c). Obviously, $S = S_c + S_n$, $E = E_c + E_n, A = A_c + A_n$, and $S + E + A + I + R = 1$. The population in compartments S, E, and A cannot determine whether they are infected with the virus. Thus, we suppose that the proportion of behavioral changes among these three groups can be considered the same, that is, $S_c/S = E_c/E = A_c/A = (S_c + E_c + A_c)/(S + E + A) = B_c$ (Assumption I).

Next, we redefine the force of disease infection as $\Theta = \beta_I I + \beta_E E_n + \rho_E \beta_E E_c + \beta_A A_n + \rho_A \beta_A A_c$, where $(\beta_I, \beta_E, \rho_E\beta_E, \beta_A, \rho_A\beta_A)$ are the effective propagation coefficients of (I, E_n, E_c, A_n, A_c). A new SEAIRS model is defined as follows:

$$\begin{cases} S_n'(t) = -\Theta S_n, \\ S_c'(t) = -q\Theta S_c, \\ E_n'(t) = \Theta S_n - \sigma E_n, \\ E_c'(t) = q\Theta S_c - \sigma E_c, \\ A_n'(t) = \varrho\sigma E_n - kA_n, \\ A_c'(t) = \varrho\sigma E_c - kA_c, \\ I'(t) = (1-\varrho)\sigma E + (1-\epsilon)kA - \gamma I, \\ R'(t) = \gamma_I I + \epsilon k A, \end{cases} \tag{2.1}$$

where $(1-\epsilon)k$ and ϵk represent the ratios of A to I and R, respectively. As the number of infected cases increases, the information index does not always rise but ultimately reaches saturation [30, 31]. Let b be a saturation constant. We reset the information index to satisfy the following equation:

$$M'(t) = \frac{aI}{1+bI} - \eta M. \tag{2.2}$$

Compared with the linear form used by Tang et al. [25], our saturated form is more realistic as it captures the natural saturation of information dissemination. It should be emphasized that $M(t)$ is a latent variable, not a directly observable indicator. Its role in the model is to capture the aggregate information effect at the population level, thereby integrating the dynamic interactions among

information propagation, risk perception, and behavioral feedback. In the following content, we will analyze the dynamics of behavioral changes. Usually, individuals will decide whether to change their behavior by comparing their interests. Assume their update strategy follows the classic Fermi update rule [20], that is, in the current round of comparison, the individual i randomly selects their nearest neighbor j to compare payoffs, and the probability of i adopting j's strategy in the next round is defined by the Fermi function [32–34] as follows:

$$W_{i\to j} = \frac{1}{1 + exp[-\zeta(f_j - f_i)]}, \tag{2.3}$$

where $f_j - f_i$ is the return difference between the two strategies, and ζ represents the individual sensitivity to the payoff differences. Generally, negative cost values can measure the size of returns for two behaviors, and they can be considered linearly related to the information function $M(t)$. Therefore, the specific payoffs of these two behaviors are expressed as follows:

$$\begin{cases} f_n = -\xi_n M(t), & \text{behavior unchanged,} \\ f_c = -\xi_c M(t) - C, & \text{behavior change,} \end{cases}$$

where C is a fixed cost paid by individuals who change their behavior, and ξ_n, ξ_c represent the cost of infection risk for individuals with two behaviors, respectively. Changing cheir behavior can reduce the risk of infection. Thus, $\xi_n > \xi_c$. Accordingly, a higher $M(t)$ increases the payoff difference $f_c - f_n = (\xi_n - \xi_c)M(t) - C$, which promotes the adoption of protective behaviors. This reduces the effective contact rates and ultimately suppresses the disease transmission. In this way, $M(t)$ serves as a bridge that links information propagation to behavioral change and epidemic dynamics.

Let $x(t)$ be the proportion of making a behavioral change at time t. According to [20], when $f_c < f_n$, all individuals in (S, E, A) who adopt behavior change strategies will learn from other individuals who do not change their behavior, and the probability of them changing their original strategy is $W_{c\to n}$. Thus, x will decrease: $x_- = x(t)(1 - x(t))W_{c\to n}$. On the contrary, when $f_c > f_n$, all individuals in (S, E, A) who do not adopt behavior change strategies will learn from others who change their behavior, and the probability of them adopting a behavior change is defined as $W_{n\to c}$. In this situation, x will increase: $x_+ = (1-x(t))x(t)W_{n\to c}$. From the above, it is easy to obtain that the evolutionary game equation for x in two-strategic games is as follows: $x(t)' = \nu(x_+ - x_-)$. Hence, the dynamics of human behavior changes can be described by $x' = \nu x(1-x)(W_{n\to c} - W_{c\to n})$, where ν is the speed of behavioral change. Following Tang et al. [25], we apply a mean-field approximation and assume a well-mixed population where the proportion of behavioral changers is identical across classes (Assumption I), thus allowing microscopic payoff comparisons to translate into the deterministic evolution of $B_c(t)$ based on the average payoff difference $(f_c - f_n)$. Combining Eq (2.3), we obtain the following:

$$
\begin{aligned}
x' &= \nu x(1-x)(W_{n\to c} - W_{c\to n}) \\
&= \nu x(1-x)\left(\frac{1}{1+\exp[-\zeta(f_c - f_n)]} - \frac{1}{1+\exp[-\zeta(f_n - f_c)]}\right) \\
&= \nu x(1-x)\left(\frac{\exp[-\zeta(f_n - f_c)] - \exp[-\zeta(f_c - f_n)]}{2+\exp[-\zeta(f_c - f_n)] + \exp[-\zeta(f_n - f_c)]}\right) \\
&= \nu x(1-x)\frac{(\exp[-\frac{\zeta}{2}(f_n - f_c)])^2 - (\exp[\frac{\zeta}{2}(f_n - f_c)])^2}{(\exp[-\frac{\zeta}{2}(f_n - f_c)] + \exp[\frac{\zeta}{2}(f_n - f_c)])^2} \\
&= \nu x(1-x)\frac{\exp[-\frac{\zeta}{2}(f_n - f_c)] - \exp[\frac{\zeta}{2}\zeta(f_n - f_c)]}{\exp[-\frac{\zeta}{2}(f_n - f_c)] + \exp[\frac{\zeta}{2}(f_n - f_c)]} \\
&= \nu x(1-x)\tanh(\frac{\zeta}{2}(f_c - f_n)) \\
&= :\nu x(1-x)\tanh(\Delta).
\end{aligned}
$$

Let τ be the time unit of behavior change. Based on the above analysis, the dynamic equation of behavior change between (S_n, E_n, A_n) and (S_c, E_c, A_c) in Model (2.1) satisfies the following:

$$
\begin{cases}
S_c'(\tau) = \begin{cases} \nu S_c(S_n + E_n + A_n)\tanh(\Delta), & \Delta < 0, \\ \nu S_n(S_c + E_c + A_c)\tanh(\Delta), & \Delta > 0. \end{cases} \\
S_n'(\tau) = \begin{cases} -\nu S_c(S_n + E_n + A_n)\tanh(\Delta), & \Delta < 0, \\ -\nu S_n(S_c + E_c + A_c)\tanh(\Delta), & \Delta > 0. \end{cases} \\
E_c'(\tau) = \begin{cases} \nu E_c(S_n + E_n + A_n)\tanh(\Delta), & \Delta < 0, \\ \nu E_n(S_c + E_c + A_c)\tanh(\Delta), & \Delta > 0. \end{cases} \\
E_n'(\tau) = \begin{cases} -\nu E_c(S_n + E_n + A_n)\tanh(\Delta), & \Delta < 0, \\ -\nu E_n(S_c + E_c + A_c)\tanh(\Delta), & \Delta > 0. \end{cases} \\
A_c'(\tau) = \begin{cases} \nu A_c(S_n + E_n + A_n)\tanh(\Delta), & \Delta < 0, \\ \nu A_n(S_c + E_c + A_c)\tanh(\Delta), & \Delta > 0. \end{cases} \\
A_n'(\tau) = \begin{cases} -\nu A_c(S_n + E_n + A_n)\tanh(\Delta), & \Delta < 0, \\ -\nu A_n(S_c + E_c + A_c)\tanh(\Delta), & \Delta > 0. \end{cases}
\end{cases}
\tag{2.4}
$$

From (2.1) and (2.4), a new model is expressed as follows:

$$
\begin{cases}
S_n'(t) = -\Theta S_n + \frac{1}{\alpha}S_n'(\tau), \\
S_c'(t) = -q\Theta S_c + \frac{1}{\alpha}S_c'(\tau), \\
E_n'(t) = \Theta S_n - \sigma E_n + \frac{1}{\alpha}E_n'(\tau), \\
E_c'(t) = q\Theta S_c - \sigma E_c + \frac{1}{\alpha}E_c'(\tau), \\
A_n'(t) = \varrho\sigma E_n - kA_n + \frac{1}{\alpha}A_n'(\tau), \\
A_c'(t) = \varrho\sigma E_c - kA_c + \frac{1}{\alpha}A_c'(\tau), \\
I'(t) = (1-\varrho)\sigma E + (1-\epsilon)kA - \gamma I, \\
R'(t) = \gamma I + \epsilon kA,
\end{cases}
\tag{2.5}
$$

where α is the scale parameter between the time unit τ of behavioral change and the time unit t of disease transmission. The two time units are related by $t = \alpha\tau$. Based on Assumption I, we have

$$\begin{aligned}\Theta &= \beta_I I + \beta_E E_n + \rho_E\beta_E E_c + \beta_A A_n + \rho_A\beta_A A_c \\ &= \beta_I I + \beta_E E\frac{E_n}{E} + \rho_E\beta_E E\frac{E_c}{E} + \beta_A A\frac{A_n}{A} + \rho_A\beta_A A\frac{A_c}{A} \\ &= \beta_I I + (\beta_E E + \beta_A A)(1 - B_c) + (\rho_E\beta_E E + \rho_A\beta_A A)B_c,\end{aligned}$$

and

$$\begin{aligned}(S_c + E_c + A_c)' &= (S + E + A)'B_c + (S + E + A)B_c' \\ &= B_c(\sigma(\varrho - 1)E - kA) + B_c'(S_c + E_c + A_c)/B_c, \\ (S_c + E_c + A_c)' &= \sigma E_c(\varrho - 1) - kA_c + \frac{\nu}{\alpha}[(S_c + E_c + A_c)(S_n + E_n + A_n)\tanh(\Delta)].\end{aligned}$$

By combining the above two equations, it can be inferred that

$$B_c' = \frac{\nu}{\alpha}B_c(1 - B_c)(S + E + A)\tanh(\Delta). \tag{2.6}$$

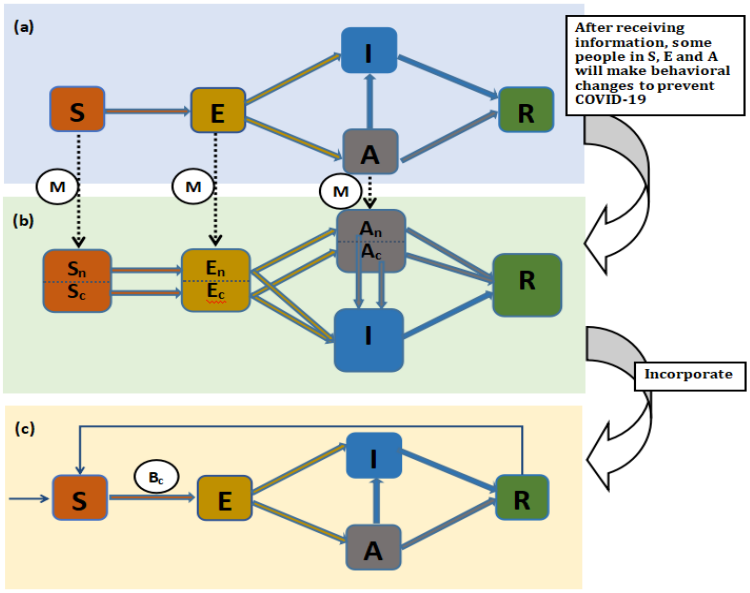

Figure 1. Flow diagram of disease transmission.

Note that $x(t)$ and $B_c(t)$ represent the same quantity: the proportion of individuals that adopt behavioral change in (S, E, A). The notation $B_c(t)$ is introduced after the mean-field approximation to emphasize its role as a macroscopic state variable in the compartmental model. $B_c(t)$ is a model-implied variable derived from the evolutionary game dynamics described by Eqs (2.3)–(2.6). It represents the proportion of individuals that adopt behavioral changes under the assumed payoff structure and the Fermi update rule, rather than being directly observable or measured from survey data. Next, we consider the case that recovered individuals may lose their immunity after some time, and ultimately incorporate Model (2.5) to obtain the following SEAIRS model:

$$\begin{cases} S' = \mu - [\beta_I I + (\beta_E E + \beta_A A)(1 - B_c) + (\rho_E \beta_E E + \rho_A \beta_A A) B_c] S (1 - B_c + q B_c) - \mu S + \delta R, \\ E' = [\beta_I I + (\beta_E E + \beta_A A)(1 - B_c) + (\rho_E \beta_E E + \rho_A \beta_A A) B_c] S (1 - B_c + q B_c) - \sigma E - \mu E, \\ A' = \varrho \sigma E - kA - \mu A, \\ I' = (1 - \varrho)\sigma E + (1 - \epsilon) kA - \gamma_I I - \mu I, \\ R' = \gamma_I I + \epsilon k A - \mu R - \delta R, \end{cases} \tag{2.7}$$

where μ denotes the susceptible populations' natural mortality and inflow rates, and δ represents the immune loss rate. Figure 1 is a simplified process to derive Model (2.7). In Figure 1(b),(c), we provide the flowcharts for Models (2.5) and (2.7), respectively. In the following, we mainly discuss some basic properties of Model (2.7).

Remark 1. *In Section 3, we treat B_c as a constant parameter to simplify the stability analysis of the disease transmission dynamics. The full dynamics of B_c (Eq (2.6)) will be incorporated in Sections 4 and 5.*

3. Main results

3.1. Positivity and boundedness of solutions

It is essential to prove that all state variables of Model (2.7) are positive and bounded at all times t. Denote $R_{+0} = [0, +\infty)$; the following results can be given.

Theorem 1. *For any given initial value $(S(0), E(0), A(0), I(0), R(0)) \in R_{+0}$, the solution of Model (2.7) satisfies $(S(t), E(t), A(t), I(t), R(t)) \in R_{+0}$ for all time $t \geq 0$.*

Proof. Let (S, E, A, I, R) be the solutions of Model (2.7) and $u(\tau) = [\beta_I I(\tau) + (\beta_E E(\tau) + \beta_A A(\tau))(1 - B_c(\tau)) + (\rho_E \beta_E E(\tau) + \rho_A \beta_A A(\tau)) B_c(\tau)](1 - B_c(\tau) + q B_c(\tau))$. According to the first equation of the system (2.7), one has the following:

$$\frac{dS}{dt} + [\beta_I I + (\beta_E E + \beta_A A)(1 - B_c) + (\rho_E \beta_E E + \rho_A \beta_A A) B_c] S (1 - B_c + q B_c) + \mu S = \mu + \delta R.$$

We multiply $\exp\{\mu t + \int_0^t u(\tau) d\tau\}$ on both sides of the above equation and obtain the following:

$$\frac{dS(t) \exp\{\mu t + \int_0^t u(\tau) d\tau\}}{dt} = \exp\{\mu t + \int_0^t u(\tau) d\tau\}(\mu + \delta R).$$

Then, taking the integral from 0 to t yields the following:

$$S(t) \exp\left\{\mu t + \int_0^t u(\tau) d\tau\right\} - S(0) = \int_0^t \exp\left\{\mu t + \int_0^x u(\tau) d\tau\right\}(\mu + \delta R) dx.$$

For any $S(0) \geq 0$, it is easy to have

$$S(t) \geq S(0) \exp\{ - \mu t - \int_0^t u(\tau) d\tau\} \geq 0.$$

Similarly, for all $t \geq 0$ and $E(0) \geq 0$, $A(0) \geq 0$, $I(0) \geq 0$, $R(0) \geq 0$, it can be shown that

$$E(t) \geq E(0)\exp\{-(\sigma+\mu)t\} \geq 0, \quad A(t) \geq A(0)\exp\{-(k+\mu)t\} \geq 0,$$
$$I(t) \geq I(0)\exp\{-(\gamma+\mu)t\} \geq 0, \quad R(t) \geq R(0)\exp\{-(\delta+\mu)t\} \geq 0.$$

To prove the boundedness of the solutions, we add all equations of System (2.7), and we get

$$(S+E+A+I+R)' = \mu - \mu(S+E+A+I+R).$$

Thus,

$$\limsup_{t\to\infty}(S(t)+E(t)+A(t)+I(t)+R(t)) \leq 1.$$

This implies $\limsup_{t\to\infty} S(t) \leq 1$, $\limsup_{t\to\infty} E(t) \leq 1$, $\limsup_{t\to\infty} A(t) \leq 1$, $\limsup_{t\to\infty} I(t) \leq 1$, and $\limsup_{t\to\infty} R(t) \leq 1$. This proof is complete.

3.2. Existence and stability of disease-free and endemic equilibria

According to the next generation matrix method [35], we obtain the basic reproduction numbers for Model (2.7) in three behavior scenarios, namely $B_c = 0$, $B_c = 1$, and $0 < B_c < 1$, as follows:

$$R_0^0 = \frac{\beta_E}{\sigma+\mu} + \frac{\beta_A\varrho\sigma}{(\sigma+\mu)(k+\mu)} + \frac{\beta_I[\varrho\sigma(1-\epsilon)k + (k+\mu)(1-\varrho)\sigma]}{(\sigma+\mu)(k+\mu)(\gamma_I+\mu)},$$
$$R_0^1 = \frac{q\rho_E\beta_E}{\sigma+\mu} + \frac{q\rho_A\beta_A\varrho\sigma}{(\sigma+\mu)(k+\mu)} + \frac{\beta_I q[\varrho\sigma(1-\epsilon)k + (k+\mu)(1-\varrho)\sigma]}{(\sigma+\mu)(k+\mu)(\gamma_I+\mu)},$$
$$R_0^c = (1 - B_c + qB_c) * \left[\frac{((1-B_c)\beta_E + \rho_E\beta_E B_c)}{\sigma+\mu} + \frac{((1-B_c)\beta_A + \rho_A\beta_A B_c)\varrho\sigma}{(\sigma+\mu)(k+\mu)} + \frac{\beta_I(\varrho\sigma(1-\epsilon)k + (k+\mu)(1-\varrho)\sigma)}{(\sigma+\mu)(k+\mu)(\gamma_I+\mu)}\right].$$

Next, we will analyze three cases based on the value of B_c.

Case (i): If all susceptible, exposed, and asymptomatic infected individuals in System (2.7) do not change their behavior ($B_c = 0$), then Model (2.7) can be simplified as follows:

$$\begin{cases} S'(t) = \mu - (\beta_I I + \beta_E E + \beta_A A)S - \mu S + \delta R, \\ E'(t) = (\beta_I I + \beta_E E + \beta_A A)S - (\sigma+\mu)E, \\ A'(t) = \varrho\sigma E - (k+\mu)A, \\ I'(t) = (1-\varrho)\sigma E + (1-\epsilon)kA - (\gamma_I+\mu)I, \\ R'(t) = \gamma_I I + \epsilon kA - (\mu+\delta)R. \end{cases} \tag{3.1}$$

Theorem 2. *(i) If $R_0^0 < 1$, then Model (3.1) has a disease-free equilibrium $E_1^0 = (1,0,0,0,0)$, which is globally asymptotically stable. (ii) If $R_0^0 > 1$, then there exists a unique endemic equilibrium $E_1^* = (S_1, E_1, A_1, I_1, R_1)$ in Model (3.1). If $R_0^0 > \max\{2\beta_E/\mu, 2\beta_A/\mu, 2\beta_I/\mu\}$, then E_1^* is locally asymptotically stable.*

Proof. The equilibrium point of System (3.1) satisfies the following equations:

$$\begin{cases} \mu - (\beta_I I + \beta_E E + \beta_A A)S - \mu S + \delta R = 0, \\ (\beta_I I + \beta_E E + \beta_A A)S - (\sigma+\mu)E = 0, \\ \varrho\sigma E - (k+\mu)A = 0, \\ (1-\varrho)\sigma E + (1-\epsilon)kA - (\gamma_I+\mu)I = 0, \\ \gamma_I I + \epsilon kA - (\mu+\delta)R = 0. \end{cases} \tag{3.2}$$

(i) When $R_0^0 < 1$, we have $I = 0$. Thus, it is easy to obtain a unique disease-free equilibrium $E_0^0 = (1, 0, 0, 0, 0)$ of Model (3.1). Next, we construct a Lyapunov function as follows:

$$V_1 = E + \frac{\beta_I I}{\gamma_I + \mu} + \frac{\beta_A(\gamma_I + \mu)A + \beta_I k(1-\epsilon)A}{(k+\mu)(\gamma_I + \mu)}.$$

Through calculation, its derivative satisfies the following:

$$\begin{aligned} V_1' &= E' + \frac{\beta_I I'}{\gamma_I + \mu} + \frac{\beta_A A'}{k+\mu} + \frac{\beta_I k(1-\epsilon)A'}{(k+\mu)(\gamma_I+\mu)} \\ &= (\beta_I I + \beta_E E + \beta_A A)S - (\sigma+\mu)E + \frac{\beta_I(1-\varrho)\sigma E + \beta_I(1-\epsilon)kA}{(\gamma_I+\mu)} - \beta_I I \\ &\quad + \frac{\beta_A \varrho\sigma E}{(k+\mu)} - \beta_A A + \frac{\beta_I k(1-\epsilon)\varrho\sigma E}{(k+\mu)(\gamma_I+\mu)} - \frac{\beta_I k(1-\epsilon)A}{(\gamma_I+\mu)}. \end{aligned}$$

By Theorem 1, it can be obtained that

$$\begin{aligned} V_1' &\le \beta_E E - (\sigma+\mu)E + \frac{\beta_I(1-\varrho)\sigma E}{(\gamma_I+\mu)} + \frac{\beta_A\varrho\sigma E}{(k+\mu)} + \frac{\beta_I k(1-\epsilon)\varrho\sigma E}{(k+\mu)(\gamma_I+\mu)} \\ &= (\sigma+\mu)E\left[\frac{\beta_E}{(\sigma+\mu)} + \frac{\beta_I(1-\varrho)\sigma}{(\gamma_I+\mu)(\sigma+\mu)} + \frac{\beta_A\varrho\sigma}{(k+\mu)(\sigma+\mu)} + \frac{\beta_I k(1-\epsilon)\varrho\sigma}{(\sigma+\mu)(k+\mu)(\gamma_I+\mu)} - 1\right] \\ &= (\sigma+\mu)E(R_0^0 - 1). \end{aligned}$$

Obviously, if $R_0^0 < 1$, then $V_1' \le 0$. Furthermore, $V_1' = 0$ only holds at the disease-free equilibrium E_0^0. According to LaSalle's invariant principle, E_0^0 is globally asymptotically stable when $R_0^0 < 1$.

(ii) According to the third equation of Eq (3.2), the endemic equilibrium $E_1^* = (S_1, E_1, A_1, I_1, R_1)$ satisfies $E_1 = (k+\mu)A_1/\varrho\sigma$. Then, we bring this equation into the fourth and fifth equations of Model (3.2) and obtain the following:

$$A_1 = \frac{\varrho(\gamma_I+\mu)I_1}{(1-\varrho)(k+\mu) + \varrho k(1-\epsilon)}, \quad R_1 = \frac{\gamma_I I_1}{(\mu+\delta)} + \frac{\epsilon k\varrho(\gamma_I+\mu)I_1}{(\mu+\delta)[(1-\varrho)(k+\mu) + \varrho k(1-\epsilon)]}.$$

From $S + E + A + I + R = 1$, we derive that $S_1 = 1 - E_1 - A_1 - I_1 - R_1 = 1 - K_1 I_1$, where

$$K_1 = \frac{\varrho\sigma(\gamma_I+\mu)(\mu+\delta) + \gamma_I\sigma[(1-\varrho)(k+\mu) + \varrho k(1-\epsilon)] + \epsilon k\varrho\sigma(\gamma_I+\mu) + (\mu+\delta)(k+\mu)(\gamma_I+\mu)}{\sigma(\mu+\delta)[(1-\varrho)(k+\mu) + \varrho k(1-\epsilon)]} + 1.$$

Substituting S_1, E_1, A_1 and I_1 in the second equation of (3.2) yields the following:

$$(1 - K_1 I_1)[\sigma((1-\varrho)(k+\mu) + \varrho k(1-\epsilon))\beta_I + \beta_E(k+\mu)(\gamma_I+\mu) + \sigma\varrho\beta_A(\gamma_I+\mu)] = (\sigma+\mu)(k+\mu)(\gamma_I+\mu).$$

By solving the equation, one has

$$\begin{aligned} I_1 &= \frac{\sigma((1-\varrho)(k+\mu) + \varrho k(1-\epsilon))\beta_I + \beta_E(k+\mu)(\gamma_I+\mu) + \sigma\varrho\beta_A(\gamma_I+\mu) - (\sigma+\mu)(k+\mu)(\gamma_I+\mu)}{K_1[\sigma((1-\varrho)(k+\mu) + \varrho k(1-\epsilon))\beta_I + \beta_E(k+\mu)(\gamma_I+\mu) + \sigma\varrho\beta_A(\gamma_I+\mu)]} \\ &= \frac{(\sigma+\mu)(k+\mu)(\gamma_I+\mu)(R_0^0 - 1)}{K_1[\sigma((1-\varrho)(k+\mu) + \varrho k(1-\epsilon))\beta_I + \beta_E(k+\mu)(\gamma_I+\mu) + \sigma\varrho\beta_A(\gamma_I+\mu)]}, \end{aligned}$$

and $S_1 = 1/R_0^0$. It is clear that $I_1 > 0$ as $R_0^0 > 1$. The Jacobian matrix of Model (3.1) at E_1^* is as follows:

$$J_1 = \begin{bmatrix} -(\beta_I I_1 + \beta_E E_1 + \beta_A A_1 + \mu) & -\beta_E S_1 & -\beta_A S_1 & -\beta_I S_1 & \delta \\ \beta_I I_1 + \beta_E E_1 + \beta_A A_1 & \beta_E S_1 - (\sigma + \mu) & \beta_A S_1 & \beta_I S_1 & 0 \\ 0 & \varrho\sigma & -(k + \mu) & 0 & 0 \\ 0 & (1 - \varrho)\sigma & (1 - \epsilon)k & -(\gamma_I + \mu) & 0 \\ 0 & 0 & \epsilon k & \gamma_I & -(\mu + \delta) \end{bmatrix}.$$

The five column Gerschgorin circles of matrix J_1 are as follows:

$$\begin{aligned} &G_1 : |\lambda + (\beta_I I_1 + \beta_E E_1 + \beta_A A_1 + \mu)| \le \beta_I I_1 + \beta_E E_1 + \beta_A A_1, \\ &G_2 : |\lambda - \beta_E S_1 + \sigma + \mu| \le \beta_E S_1 + \sigma, \\ &G_3 : |\lambda + k + \mu| \le 2\beta_A S_1 + k, \\ &G_4 : |\lambda + \gamma_I + \mu| \le 2\beta_I S_1 + \gamma_I, \\ &G_5 : |\lambda + \mu + \delta| \le \delta. \end{aligned}$$

By the Gale circle theorem, all five eigenvalues of matrix J_1 are in $\bigcup_{i=1}^{5} G_i$. If $R_0^0 > \max\{2\beta_E/\mu, 2\beta_A/\mu, 2\beta_I/\mu\}$ holds, we have the following:

$$\begin{aligned} &-2(\beta_I I_1 + \beta_E E_1 + \beta_A A_1) - \mu \le \lambda \le -\mu < 0, \\ &-2\sigma - \mu \le \lambda \le 2\beta_E S_1 - \mu < 0, \\ &-2\beta_A S_1 - 2k - \mu \le \lambda \le 2\beta_A S_1 - \mu < 0, \\ &-2\beta_I S_1 - 2\gamma_I - \mu \le \lambda \le 2\beta_I S_1 - \mu < 0, \\ &-2\delta - \mu \le \lambda \le -\mu < 0. \end{aligned}$$

According to the Routh-Hurwitz theorem, E_1^* is locally asymptotically stable.

Case (ii): When all susceptible, exposed, and asymptomatic infected in the Model (2.7) change their behavior ($B_c = 1$), Model (2.7) can be rewritten as follows:

$$\begin{cases} S'(t) = \mu - q(\beta_I I + \rho_E\beta_E E + \rho_A\beta_A A)S - \mu S + \delta R, \\ E'(t) = q(\beta_I I + \rho_E\beta_E E + \rho_A\beta_A A)S - (\sigma + \mu)E, \\ A'(t) = \varrho\sigma E - (k + \mu)A, \\ I'(t) = (1 - \varrho)\sigma E + (1 - \epsilon)kA - (\gamma_I + \mu)I, \\ R'(t) = \gamma_I I + \epsilon kA - (\mu + \delta)R. \end{cases} \tag{3.3}$$

Theorem 3. *(i) If $R_0^1 < 1$, then Model (3.3) has a disease-free equilibrium $E_2^0 = (1, 0, 0, 0, 0)$, which is globally asymptotically stable. (ii) If $R_0^1 > 1$, then there exists a unique endemic equilibrium $E_2^* = (S_2, E_2, A_2, I_2, R_2)$ in Model (3.3). If $R_0^1 > \max\{2q\rho_E\beta_E/\mu, 2q\rho_A\beta_A/\mu, 2q\beta_I/\mu\}$, then E_2^* is locally asymptotically stable.*

Proof. The equilibrium point of System (3.4) satisfies the following equations:

$$\begin{cases} \mu - q(\beta_I I + \rho_E\beta_E E + \rho_A\beta_A A)S - \mu S + \delta R = 0, \\ q(\beta_I I + \rho_E\beta_E E + \rho_A\beta_A A)S - (\sigma + \mu)E = 0, \\ \varrho\sigma E - (k + \mu)A = 0, \\ (1 - \varrho)\sigma E + (1 - \epsilon)kA - (\gamma_I + \mu)I = 0, \\ \gamma_I I + \epsilon kA - (\mu + \delta)R = 0. \end{cases} \tag{3.4}$$

(i) When $R_0^1 < 1$, we have $I = 0$. Thus, it is easy to obtain a unique disease-free equilibrium $E_2^0 = (1, 0, 0, 0, 0)$ of Model (3.3). Define a Lyapunov function as follows:

$$V_3 = E + \frac{q\beta_I I}{\gamma_I + \mu} + \frac{q\rho_A\beta_A(\gamma_I + \mu)A + q\beta_I k(1-\epsilon)A}{(k+\mu)(\gamma_I+\mu)}.$$

Based on (3.3), we can derive that

$$\begin{aligned} V_3' &= E' + \frac{q\beta_I I'}{\gamma_I+\mu} + \frac{q\rho_A\beta_A A'}{k+\mu} + \frac{q\beta_I k(1-\epsilon)A'}{(k+\mu)(\gamma_I+\mu)} \\ &= q(\beta_I I + \rho_E\beta_E E + \rho_A\beta_A A)S - (\sigma+\mu)E + \frac{q\beta_I(1-\varrho)\sigma E + q\beta_I(1-\epsilon)kA}{(\gamma_I+\mu)} \\ &\quad - q\beta_I I + \frac{q\rho_A\beta_A\varrho\sigma E}{(k+\mu)} - q\rho_A\beta_A A + \frac{q\beta_I k(1-\epsilon)\varrho\sigma E}{(k+\mu)(\gamma_I+\mu)} - \frac{q\beta_I k(1-\epsilon)A}{(\gamma_I+\mu)}. \end{aligned}$$

By applying $S \le 1$, we have the following:

$$\begin{aligned} V_3' &\le q\rho_E\beta_E E - (\sigma+\mu)E + \frac{q\beta_I(1-\varrho)\sigma E}{(\gamma_I+\mu)} + \frac{q\rho_A\beta_A\varrho\sigma E}{(k+\mu)} + \frac{q\beta_I k(1-\epsilon)\varrho\sigma E}{(k+\mu)(\gamma_I+\mu)} \\ &= (\sigma+\mu)E\left[\frac{q\rho_E\beta_E}{(\sigma+\mu)} + \frac{q\beta_I(1-\varrho)\sigma}{(\gamma_I+\mu)(\sigma+\mu)} + \frac{q\rho_A\beta_A\varrho\sigma}{(k+\mu)(\sigma+\mu)} + \frac{q\beta_I k(1-\epsilon)\varrho\sigma}{(\sigma+\mu)(k+\mu)(\gamma_I+\mu)} - 1\right] \\ &= (\sigma+\mu)E(R_0^1 - 1). \end{aligned}$$

From the above equation, if $R_0^1 < 1$ holds, then $V_3' \le 0$. $V_3' = 0$ only holds at the disease-free equilibrium point E_2^0. By LaSalle's invariant principle, E_2^0 is globally asymptotically stable.

(ii) Similar to E_1^*, we obtain the positive equilibrium $E_2^* = (S_2, E_2, A_2, I_2, R_2)$ of Model (3.3), where

$$E_2 = \frac{(k+\mu)A_2}{\varrho\sigma}, A_2 = \frac{\varrho(\gamma_I+\mu)I_2}{(1-\varrho)(k+\mu)+\varrho k(1-\epsilon)}, R_2 = \frac{\gamma_I I_2}{(\mu+\delta)} + \frac{\epsilon k\varrho(\gamma_I+\mu)I_2}{(\mu+\delta)[(1-\varrho)(k+\mu)+\varrho k(1-\epsilon)]},$$

$$\begin{aligned} I_2 &= \frac{q\sigma((1-\varrho)(k+\mu)+\varrho k(1-\epsilon))\beta_I + q\rho_E\beta_E(k+\mu)(\gamma_I+\mu) + q\rho_A\sigma\varrho\beta_A(\gamma_I+\mu) - (\sigma+\mu)(k+\mu)(\gamma_I+\mu)}{K_1[q\sigma((1-\varrho)(k+\mu)+\varrho k(1-\epsilon))\beta_I + q\rho_E\beta_E(k+\mu)(\gamma_I+\mu) + q\rho_A\sigma\varrho\beta_A(\gamma_I+\mu)]} \\ &= \frac{(\sigma+\mu)(k+\mu)(\gamma_I+\mu)(R_0^1-1)}{K_1[q\sigma((1-\varrho)(k+\mu)+\varrho k(1-\epsilon))\beta_I + q\rho_E\beta_E(k+\mu)(\gamma_I+\mu) + q\rho_A\sigma\varrho\beta_A(\gamma_I+\mu)]}, \end{aligned}$$

and $S_2 = 1 - E_2 - A_2 - I_2 - R_2 = 1 - K_1 I_2 = 1/R_0^1$. From the expression of I_2, we can easily see that $I_2 > 0$ as $R_0^1 > 1$. The Jacobian matrix J_2 of Model (3.3) at E_2^* is formed by the following:

$$J_2 = \begin{bmatrix} -q(\beta_I I_2 + \rho_E\beta_E E_2 + \rho_A\beta_A A_2) - \mu & -q\rho_E\beta_E S_2 & -q\rho_A\beta_A S_2 & -q\beta_I S_2 & \delta \\ q(\beta_I I_2 + \rho_E\beta_E E_2 + \rho_A\beta_A A_2) & q\rho_E\beta_E S_2 - (\sigma+\mu) & q\rho_A\beta_A S_2 & q\beta_I S_2 & 0 \\ 0 & \varrho\sigma & -(k+\mu) & 0 & 0 \\ 0 & (1-\varrho)\sigma & (1-\epsilon)k & -(\gamma_I+\mu) & 0 \\ 0 & 0 & \epsilon k & \gamma_I & -(\mu+\delta) \end{bmatrix}.$$

The five column Gerschgorin circles of matrix J_2 are as follows:

$$\begin{aligned} &H_1 : |\lambda + q(\beta_I I_2 + \rho_E\beta_E E_2 + \rho_A\beta_A A_2) + \mu| \le q(\beta_I I_2 + \rho_E\beta_E E_2 + \rho_A\beta_A A_2), \\ &H_2 : |\lambda - q\rho_E\beta_E S_2 + \sigma + \mu| \le q\rho_E\beta_E S_2 + \sigma, \\ &H_3 : |\lambda + k + \mu| \le 2q\rho_A\beta_A S_2 + k, \\ &H_4 : |\lambda + \gamma_I + \mu| \le 2q\beta_I S_2 + \gamma_I, \\ &H_5 : |\lambda + \mu + \delta| \le \delta. \end{aligned}$$

Therefore, all five eigenvalues of matrix J_2 are in $\bigcup_{i=1}^{5} H_i$. If $R_0^1 > \max\{2q\rho_E\beta_E/\mu, 2q\rho_A\beta_A/\mu, 2q\beta_I/\mu\}$ holds, then we obtain the following:

$$\begin{aligned}
&-2q(\beta_I I_2 + \rho_E\beta_E E_2 + \rho_A\beta_A A_2) - \mu \le \lambda \le -\mu < 0,\\
&-2\sigma - \mu \le \lambda \le 2q\rho_E\beta_E S_2 - \mu < 0,\\
&-2q\rho_A\beta_A S_2 - 2k - \mu \le \lambda \le 2q\rho_A\beta_A S_2 - \mu < 0,\\
&-2q\beta_I S_2 - 2\gamma_I - \mu \le \lambda \le 2q\beta_I S_2 - \mu < 0,\\
&-2\delta - \mu \le \lambda \le -\mu < 0.
\end{aligned}$$

By the Routh-Hurwitz theorem, E_2^* is locally asymptotically stable.

Case (iii): $0 < B_c < 1$. In this case, B_c is the proportion of individuals who adopt behavioral changes in (S, E, A). Denote the following:

$$K_2 = \frac{(\mu+\delta)(k+\mu)(\gamma_I+\mu) + \sigma\varrho(\mu+\delta)(\gamma_I+\mu) + (\mu+\delta+\sigma\gamma_I)[(1-\varrho)(k+\mu)+\varrho k(1-\epsilon)] + \sigma\epsilon k\varrho(\gamma_I+\mu)}{(\mu+\delta)\sigma[(1-\varrho)(k+\mu)+\varrho k(1-\epsilon)]}.$$

Theorem 4. *(i) If $R_0^c < 1$, then Model (2.7) has a disease-free equilibrium $E_3^0 = (1, 0, 0, 0, 0)$, which is globally asymptotically stable. (ii) If $R_0^c > 1$, then there exists a unique endemic equilibrium $E_3^* = (S_3, E_3, A_3, I_3, R_3)$ in Model (2.7). In addition, E_3^* is locally asymptotically stable whenever R_0^c is larger than the maximum listed below:*

$$R_0^c > \max\left\{\frac{2[\beta_E(1-B_c)+\rho_E\beta_E B_c](1-B_c+qB_c)}{\mu}, \frac{2[\beta_A(1-B_c)+\rho_A\beta_A B_c](1-B_c+qB_c)}{\mu}, \frac{2\beta_I(1-B_c+qB_c)}{\mu}\right\}.$$

Proof. (i) When $R_0^c < 1$, we have $I = 0$. Thus, the unique disease-free equilibrium $E_3^0 = (1, 0, 0, 0, 0)$. Construct a Lyapunov function as follows:

$$V_5 = E + \frac{(1-B_c+qB_c)\beta_I I}{\gamma_I+\mu} + \frac{(1-B_c+qB_c)[(\beta_A(1-B_c)+\rho_A\beta_A B_c)(\gamma_I+\mu)+\beta_I k(1-\epsilon)]A}{(k+\mu)(\gamma_I+\mu)}.$$

Based on (3.3), we have the following:

$$\begin{aligned}
V_5' &= E' + \frac{(1-B_c+qB_c)\beta_I I'}{\gamma_I+\mu} + \frac{(1-B_c+qB_c)[(\beta_A(1-B_c)+\rho_A\beta_A B_c)(\gamma_I+\mu)+\beta_I k(1-\epsilon)]A'}{(k+\mu)(\gamma_I+\mu)}.\\
&= [\beta_I I + (\beta_E E + \beta_A A)(1-B_c) + (\rho_E\beta_E E + \rho_A\beta_A A)B_c]S(1-B_c+qB_c) - (\sigma+\mu)E\\
&\quad + \frac{(1-B_c+qB_c)\beta_I[(1-\varrho)\sigma E + (1-\epsilon)kA - (\gamma_I+\mu)I]}{(\gamma_I+\mu)}\\
&\quad + \frac{(1-B_c+qB_c)[(\beta_A(1-B_c)+\rho_A\beta_A B_c)(\gamma_I+\mu)+\beta_I k(1-\epsilon)][\varrho\sigma E - (k+\mu)A]}{(k+\mu)(\gamma_I+\mu)}.
\end{aligned}$$

According to $S \le 1$ and $1 - B_c \le 1$, it can be inferred that

$$\begin{aligned}
V_5' &\le (1-B_c+qB_c)(1-B_c)\beta_E E + (1-B_c+qB_c)B_c\rho_E\beta_E E - (\sigma+\mu)E\\
&\quad + \frac{(1-B_c+qB_c)[(\beta_A(1-B_c)+\rho_A\beta_A B_c)(\gamma_I+\mu)+\beta_I k(1-\epsilon)]\varrho\sigma E}{(k+\mu)(\gamma_I+\mu)} + \frac{(1-B_c+qB_c)\beta_I(1-\varrho)\sigma E}{(\gamma_I+\mu)}\\
&= (\sigma+\mu)E(R_0^c - 1).
\end{aligned}$$

Obviously, $V_5' \leq 0$ when $R_0^c < 1$, and $V_5' = 0$ only holds at the disease-free equilibrium point E_3^0. By LaSalle's invariant principle, E_3^0 is globally asymptotically stable.

(ii) From the Eq (2.7), we conclude that the endemic equilibrium $E_3^* = (S^*, E^*, A^*, I^*, R^*)$ satisfies the following equations:

$$E^* = \frac{(k+\mu)A^*}{\varrho\sigma},\ A^* = \frac{\varrho(\gamma_I+\mu)I^*}{(1-\varrho)(k+\mu)+\varrho k(1-\epsilon)},\ R^* = \frac{\gamma_I I^*}{(\mu+\delta)} + \frac{\epsilon k\varrho(\gamma_I+\mu)I^*}{(\mu+\delta)[(1-\varrho)(k+\mu)+\varrho k(1-\epsilon)]},$$

and $S^* = 1 - E^* - A^* - I^* - R^* = 1 - K_2 I^*$. Substituting S^*, E^*, A^*, and R^* into the second equation, we have the following:

$$S^*(1-B_c+qB_c)[\beta_I I^* + (\beta_E E^* + \beta_A A^*)(1-B_c) + (\rho_E\beta_E E^* + \rho_A\beta_A A^*)B_c] - (\sigma+\mu)E^* = 0.$$

By directly solving the above algebraic equation, we can obtain $I^* = (R_0^c - 1)/K_2 R_0^c$ and $S^* = 1/R_0^c$. Note that $I^* > 0$ for $R_0^c > 1$. The Jacobian matrix J_3 of Model (2.7) at E_3^* is as follows:

$$J_3 = \begin{bmatrix} -\Delta_1 - \mu & -\Delta_2(1-B_c+qB_c) & -\Delta_3(1-B_c+qB_c) & -\beta_I S_3(1-B_c+qB_c) & \delta \\ \Delta_1 & \Delta_2(1-B_c+qB_c) - (\sigma+\mu) & \Delta_3(1-B_c+qB_c) & \beta_I S_3(1-B_c+qB_c) & 0 \\ 0 & \varrho\sigma & -(k+\mu) & 0 & 0 \\ 0 & (1-\varrho)\sigma & (1-\epsilon)k & -(\gamma_I+\mu) & 0 \\ 0 & 0 & \epsilon k & \gamma_I & -(\mu+\delta) \end{bmatrix},$$

where $\Delta_1 = [\beta_I I_3 + (\beta_E E_3 + \beta_A A_3)(1-B_c) + (\rho_E\beta_E E_3 + \rho_A\beta_A A_3)B_c](1-B_c+qB_c)$, $\Delta_2 = [\beta_E(1-B_c) + \rho_E\beta_E B_c]S_3$, and $\Delta_3 = [\beta_A(1-B_c) + \rho_A\beta_A B_c]S_3$. The five column Gerschgorin circles of matrix J_3 are as follows:

$$\begin{aligned} &D_1 : |\lambda + \Delta_1 + \mu| \leq \Delta_1, \\ &D_2 : |\lambda - \Delta_2(1-B_c+qB_c) + \sigma + \mu| \leq \Delta_2(1-B_c+qB_c) + \sigma, \\ &D_3 : |\lambda + k + \mu| \leq 2\Delta_3(1-B_c+qB_c) + k, \\ &D_4 : |\lambda + \gamma_I + \mu| \leq 2\beta_I S_3(1-B_c+qB_c) + \gamma_I, \\ &D_5 : |\lambda + \mu + \delta| \leq \delta. \end{aligned}$$

Therefore, all five eigenvalues of matrix J_3 are in $\bigcup_{i=1}^5 D_i$. If

$$R_0^c > \max\left\{\frac{2[\beta_E(1-B_c)+\rho_E\beta_E B_c](1-B_c+qB_c)}{\mu}, \frac{2[\beta_A(1-B_c)+\rho_A\beta_A B_c](1-B_c+qB_c)}{\mu}, \frac{2\beta_I(1-B_c+qB_c)}{\mu}\right\}$$

holds, than we can derive the following result:

$$\begin{aligned} &-2\Delta_1 - \mu \leq \lambda \leq -\mu < 0, \\ &-2\sigma - \mu \leq \lambda \leq 2\Delta_2(1-B_c+qB_c) - \mu < 0, \\ &-2\Delta_3(1-B_c+qB_c) - 2k - \mu \leq \lambda \leq 2\Delta_3(1-B_c+qB_c) - \mu < 0, \\ &-2\beta_I S_3(1-B_c+qB_c) - 2\gamma_I - \mu \leq \lambda \leq 2\beta_I S_3(1-B_c+qB_c) - \mu < 0, \\ &-2\delta - \mu \leq \lambda \leq -\mu < 0. \end{aligned}$$

By the Routh-Hurwitz theorem, E_3^* is locally asymptotically stable.

4. Numerical simulations

This section provides numerical simulations to illustrate the theoretical results. We use the classical fourth-order Runge-Kutta method to obtain the discretization equations of the deterministic Model (2.7). We provide the following example to intuitively express the impact of behavioral changes in susceptible, exposed, and asymptomatic infected on disease transmission within the model.

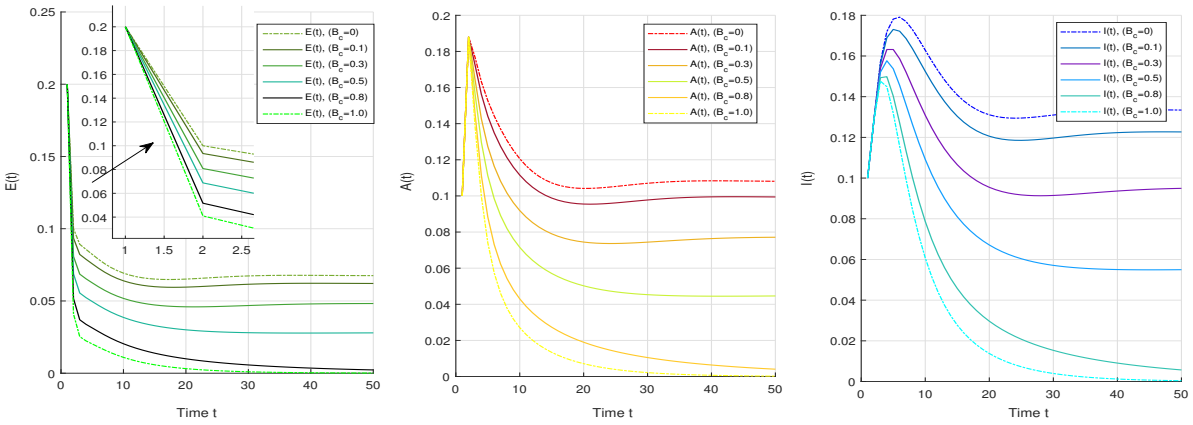

Figure 2. The variation curves of $E(t)$, $A(t)$, and $I(t)$ under different B_c.

Example 1. *Take* $B_c = (0, 0.1, 0.3, 0.5, 0.7, 1)$ *and* $(\mu, \beta_I, \beta_A, \beta_E, \delta, \sigma, k, \gamma_I, \varrho, \epsilon, \rho_A, \rho_E, q) = (0.1, 0.4, 0.4, 0.4, 0.05, 0.8, 0.3, 0.2, 0.8, 0.1, 0.9, 0.8, 0.3)$. *Figure 2 shows that the number of* $E(t), A(t)$, *and* $I(t)$ *in Model (2.7) decreases with the increase of* B_c. *Within the model framework, increasing behavioral changes leads to a reduction in the spread of diseases.*

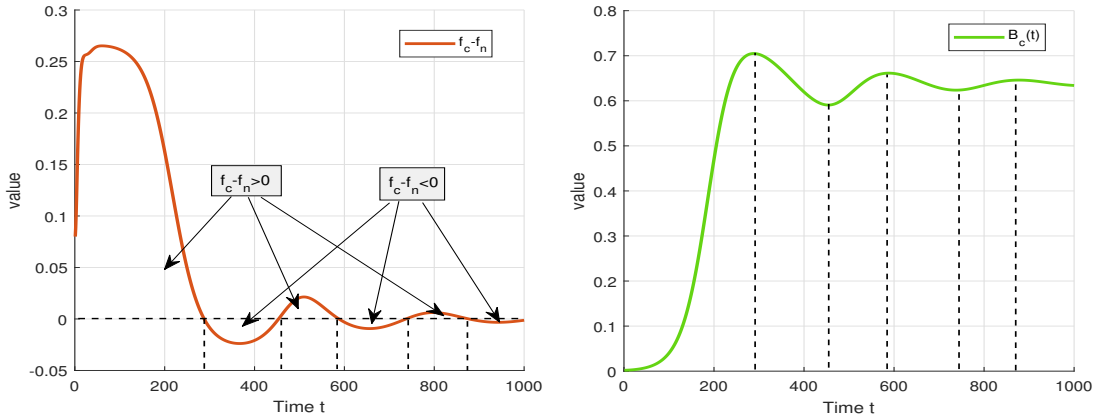

Figure 3. The variation curves of $f_c - f_n$ and $B_c(t)$.

Whether susceptible, exposed, and asymptomatic infected individuals in Model (2.7) adopt behavioral changes depends on the return difference $f_c - f_n$ between these two behaviors. We provide Example 2 to verify.

Example 2. *Assume that* $(a, b, \nu/\alpha, \eta, \zeta, \xi_n, \xi_c, C) = (0.48, 0.3, 15, 0.08, 0.025, 0.5, 0.1, 0.04)$, $(S(0), E(0), A(0), I(0), R(0), M(0), B_c(0)) = (0.5, 0.2, 0.1, 0, 1, 0.1, 0.3, 0.002)$, *and the remaining parameter values are shown in Example 1. From Figure 3, it can be seen that when* $f_c > f_n$, $B_c(t)$ *increases, while* $B_c(t)$ *decreases when* $f_c < f_n$. *This result indicates that increasing the difference in returns* $f_c - f_n$ *can effectively promote behavior changes in susceptible, exposed, and asymptomatic infected.*

In the following example, we analyze the impact of some key parameters on the difference in returns $f_c - f_n$ between these two behaviors.

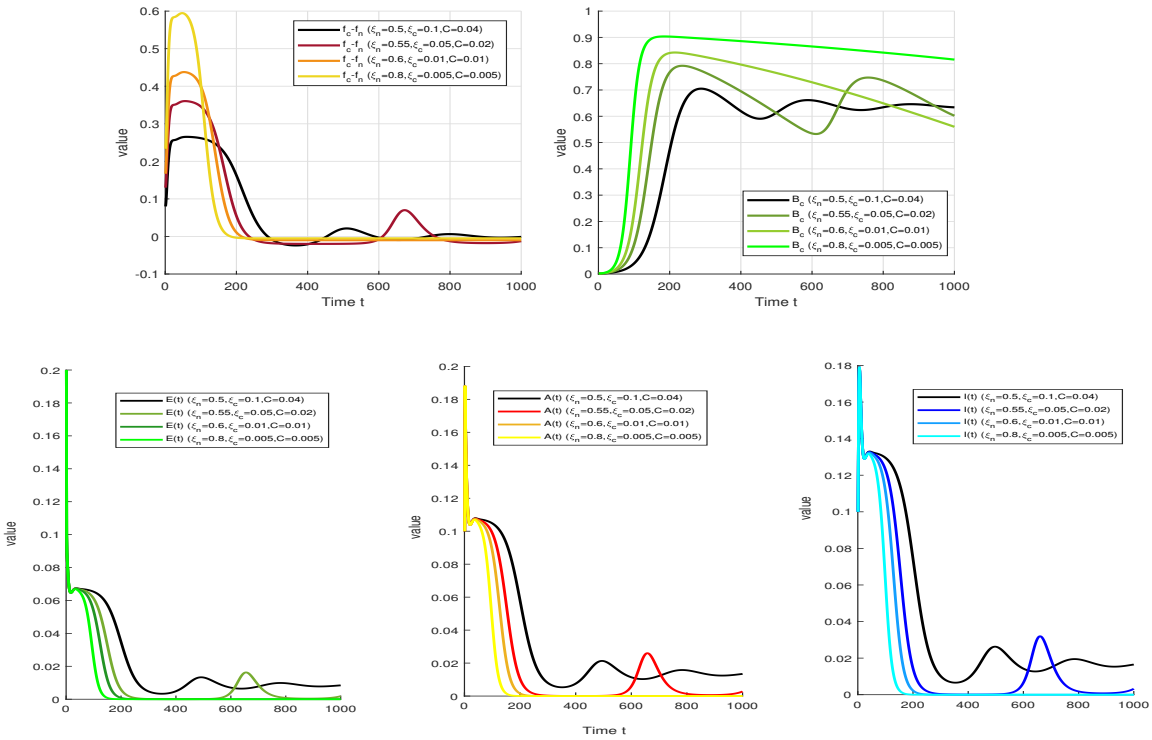

Figure 4. The variation curves of $f_c - f_n$, $B_c(t)$ and $(E(t), A(t) , I(t))$ under different ξ_n, ξ_c, and C.

Example 3. *Assume that the parameter values are the same as in Example 2. The variation curves of* $f_c - f_n$, $B_c(t)$, *and* $(E(t), A(t) , I(t))$ *under different* (ξ_n, ξ_c, C) *are shown in Figure 4. Within the model, increasing* ξ_n *or decreasing* ξ_c *and* C *leads to an increase in* $f_c - f_n$ *and* $B_c(t)$, *and a decrease in* $(E(t), A(t), I(t))$. *According to the model, adjusting the parameter values* (ξ_n, ξ_c, C) *reduces the infection levels, thus suggesting a theoretical pathway for disease control.*

Special Note: The parameter values in Examples 1–3 are theoretically chosen to clearly illustrate the model's qualitative behavior under different scenarios, rather than to fit any specific real-world data.

5. COVID-19 epidemic

In this part, we consider the cases of reported COVID-19 in Romania from July 28 to December 8, 2021. The daily new infection data shown in Figure 5 are from https://ourworldindata.org/. We divide

the time of the COVID-19 epidemic into two phases, namely, July 28 to October 15 and October 16 to December 8, 2021. According to https://ourworldindata.org/, the total population of Romania in 2021 was 19,328,558. Assume that at the beginning of the two stages, the number of $E(t)$ is 200 and 800, the $A(t)$ is 100 and 400, and the $R(t)$ is 1000 and 2000. Take $B_c(0) = 0.001$, 0.9999, and $M(0) = 1000$, 20,000. In addition, the daily new infections on July 28 and October 16, 2021, were 175 and 15,828, respectively. Thus, the initial values $(S(0), E(0), A(0), I(0), R(0), B_c(0), M(0))$ for the two stages are (19,327,083, 200, 100, 175, 1000, 0.001, 1000) and (19,309,530, 800, 400, 15,828, 2000, 0.9999, 20,000), respectively. We use the least-square method to fit the model with accurate data. Tables 1 and 2 list the estimated values of the parameters. (It should be noted that the fitting procedure in this section is intended to illustrate the model's behavior rather than to perform rigorous statistical inference. The fitting data are limited to the daily new cases of symptomatic infected individuals $I(t)$; the initial values of the other compartments are based on assumptions. Due to the high-dimensional parameter structure of the model and the use of only a single incidence time series, the parameter estimates are not uniquely identifiable; different parameter combinations may generate highly similar epidemic trajectories. Therefore, the estimated values in Tables 1 and 2 should be regarded as illustrative rather than as precise estimates of real-world epidemiological parameters.) Figure 6 shows the two-stage fitting curves for real data. The $M(t)$ curve in Figure 7(a) is the theoretical trajectory of the model-generated information index, and the $B_c(t)$ curve in Figure 7(b) is a theoretical trajectory obtained from Eq (2.6). Figure 7(c) depicts the thresholds (R_0^c, R_0^0, R_0^1) in the two phases. From Figure 7(a)–(c), we observe three results. (i) In the first phase (disease ascending period), both $M(t)$ and $B_c(t)$ increase with the increase of $I(t)$; additionally, an increase in $B_c(t)$ leads to a decrease in R_0^c, as shown in Figure 7(c). In the second phase (disease decline period), $B_c(t)$ rises slowly, and R_0^c decreases gradually. (although the observed changes are small in magnitude, they are directionally informative). (ii) The relationship between R_0^c, R_0^0, and R_0^1 is $R_0^0 \geq R_0^c \geq R_0^1$, which means that behavioral changes can reduce the basic regeneration number.

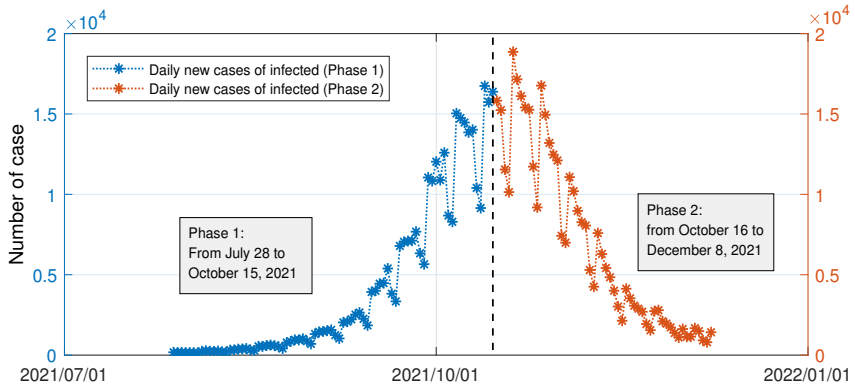

Figure 5. The numbers of new infected in Romania, from July 28 to December 8, 2021.

Next, we take the model's parameter values as the estimated values for the first phase in Table 1. It should be emphasized that the following discussion is solely based on the model's theoretical framework. Figure 8(a)–(c) shows the theoretical trajectories of $M(t)$, $B_c(t)$, and (R_0^c, R_0^0, R_0^1) computed from the model under different values of η, a, and C. The model results indicate that under the assumed conditions, increasing a or decreasing the decay rate η and the behavioral cost C leads to

higher theoretical values of $M(t)$ and $B_c(t)$, and a lower R_0^c. Taking the second stage parameter estimation values as an example, Figure 9(a) depicts the values of $E(t)$ and $I(t)$ at different β_I, β_E, and γ_I. It can be seen that reducing the contact rates β_I and β_E or increasing disease cure rate γ_I is beneficial for disease control.

It should be further noted that the large differences in fitted parameter values between the two phases should not be interpreted as literal epidemiological regime shifts, as they likely reflect a combination of behavioral, reporting, and modeling simplifications. Comparisons should focus on qualitative trends rather than absolute values. Moreover, behavioral dynamics are governed by the payoff difference $f_c - f_n$. Given the definitions $f_n = -\xi_n M(t)$ and $f_c = -\xi_c M(t) - C$, the parameters ξ_n, ξ_c, C, and $M(t)$ are not independently identifiable, as they collectively form a composite behavioral driver. Therefore, individual fitted values of these parameters should not be over-interpreted.

Table 1. The estimated values of model parameters in the first phase.

Parameters	Initial values	Estimated values	Parameters	Initial values	Estimated values
β_I	2.1200e−3	0.4086	γ_I	0.2640	0.7700
β_E	0.0031	0.2947	a	0.3000	9.7143
β_A	0.0501	0.3022	b	5.0000	3.0028
ρ_A	0.5320	0.5048	ν/α	0.8000	26.6164
ρ_E	0.1400	0.8590	ζ	3.1200e−3	0.8875
δ	2.1300e−3	0.3073	ξ_n	0.2000	0.8571
q	0.0400	0.9557	ξ_c	0.0110	0.1278
σ	0.0040	0.3942	C	1.0000e−6	5.7130e−5
ϱ	0.3100	0.0089	η	0.3200	0.0322
k	0.3310	0.9970	μ	0.0000	0.0202
ϵ	0.1310	0.0026	-	-	-

Table 2. The estimated values of model parameters in second phase.

Parameters	Initial values	Estimated values	Parameters	Initial values	Estimated values
β_I	0.2111	2.2892e−9	γ_I	0.2640	0.0830
β_E	0.0203	0.6200	a	0.3000	9.6068
β_A	5.5100e−3	0.8244	b	3.3690	2.5467
ρ_A	0.0140	0.8900	ν/α	0.8000	20.1265
ρ_E	0.1600	0.9999	ζ	3.1200e−3	0.6366
δ	0.1113	0.8099	ξ_n	0.2000	0.9809
q	0.5400	0.9420	ξ_c	0.0110	0.5536
σ	0.0040	0.7099	C	0.2312	8.2649e−5
ϱ	0.6310	6.0757e−9	η	0.6200	0.4706
k	0.3310	0.1425	μ	0.0000	3.2192e−8
ϵ	0.1310	1.2357e−6	-	-	-

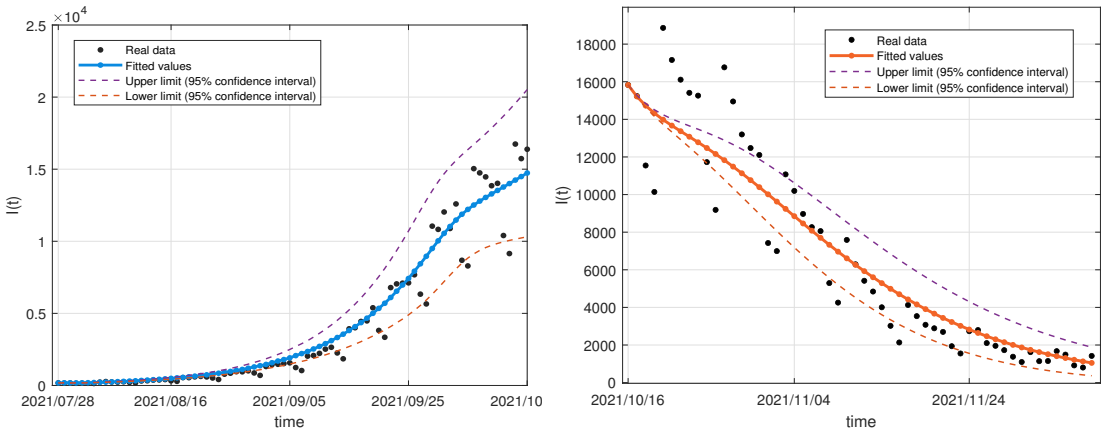

(a) (b)

Figure 6. The real data and two fitted curves of Romania's new symptomatic infected cases from July 28 to December 8, 2021.

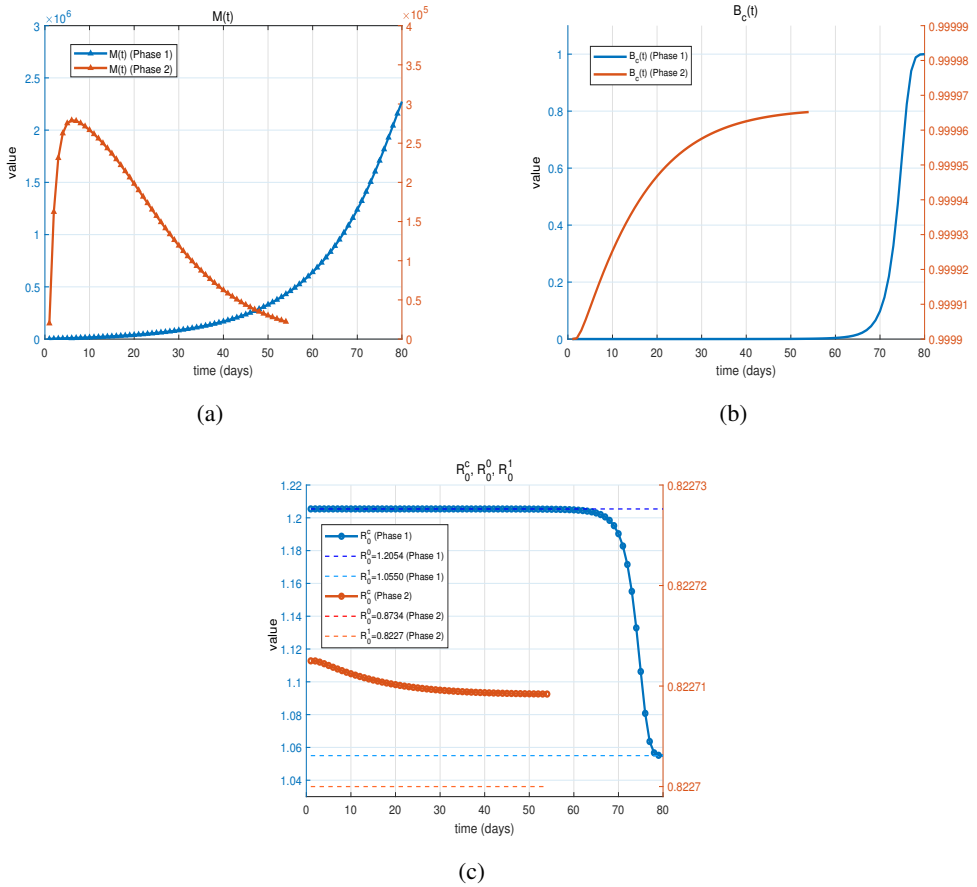

(a) (b)

(c)

Figure 7. (a) shows the theoretical curves of the model-generated information index $M(t)$ in two phases, (b) shows the theoretical trajectories of $B_c(t)$ in two phases, and (c) describes the values of (R_0^0, R_0^1, R_0^c) in two phases.

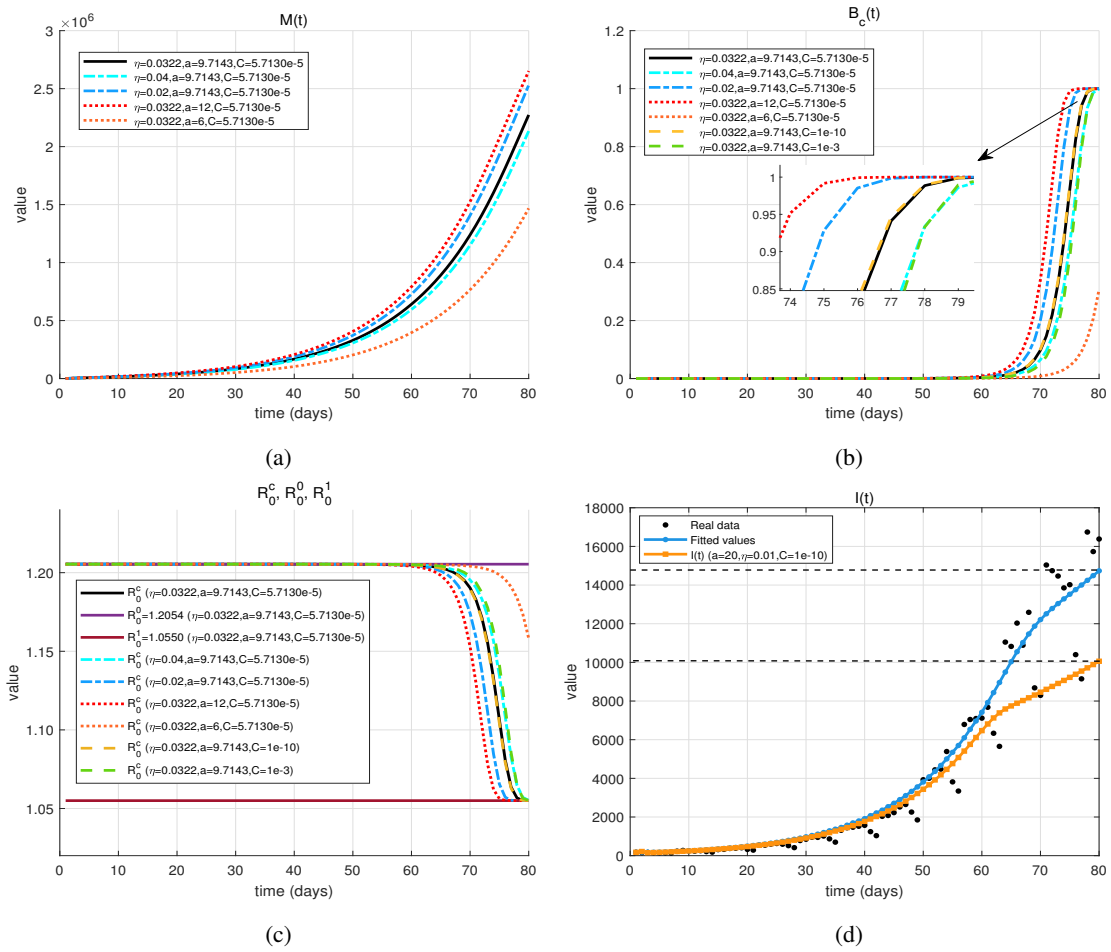

Figure 8. Theoretical variation curves of the model-generated information index $M(t)$, $B_c(t)$, $I(t)$, and the thresholds (R_0^0, R_0^1, R_0^c) under different (η, a, C) in Phase 1.

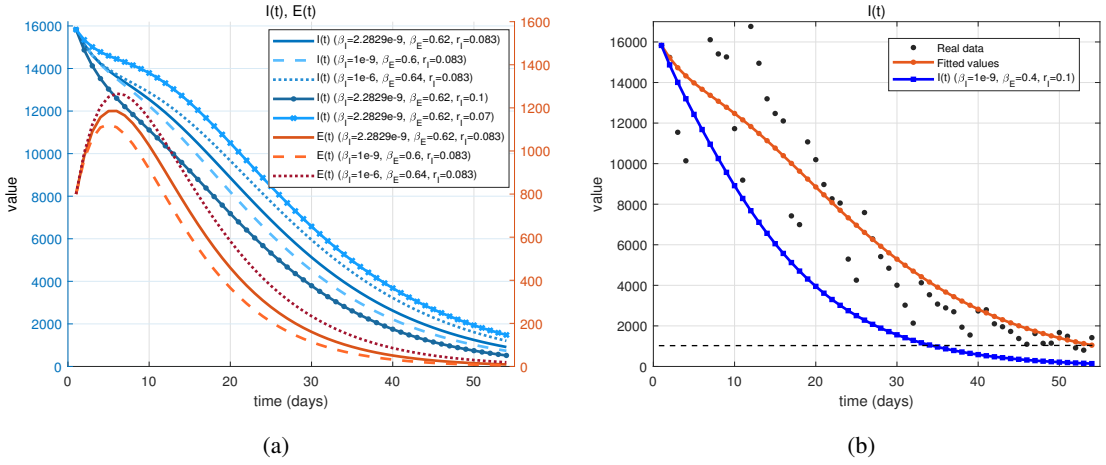

Figure 9. The variation curves of $I(t)$ and $E(t)$ under different $\beta_I, \beta_E, \gamma_I$ in the Phase 2.

6. Conclusions

This paper established a new SEAIRS model to study the impact of human behavior changes on the COVID-19 epidemic. Our Model (2.7) improves the model proposed by Tang et al. (1.1) [25], which is mainly reflected in the following two aspects: (i) the role of exposed individuals in the spread of epidemics has been considered; and (ii) improved the form of the information function. As a mechanistic and theoretical study, the following findings are analytical insights derived from model simulations, and not directly implementable operational prescriptions.

We obtained the positivity and boundedness of the solution for Model (2.7) and then discussed the existence and stability properties of equilibrium points for Model (2.7) in three situations ($B_c = 0$, $B_c = 1, 0 < B_c < 1$). The results are summarized as follows. (i) $B_c = 0$: when $R_0^0 < 1$, Model (3.1) has a unique disease-free equilibrium E_1^0, which is globally asymptotically stable; and When $R_0^0 > 1$, Model (3.1) has a unique endemic disease equilibrium E_1^*, and if $R_0^0 > \max\{2\beta_E/\mu, 2\beta_A/\mu, 2\beta_I/\mu\}$, then E_1^* is locally asymptotically stable. (ii) $B_c = 1$: when $R_0^1 < 1$, Model (3.3) has a unique disease-free equilibrium E_2^0 and E_2^0 is globally asymptotically stable; when $R_0^1 > 1$, Model (3.3) has a unique endemic disease equilibrium E_2^*, and if $R_0^1 > \max\{2q\rho_E\beta_E/\mu, 2q\rho_A\beta_A/\mu, 2q\beta_I/\mu\}$, then E_2^* is locally asymptotically stable. (iii) $0 < B_c < 1$: when $R_0^c < 1$, Model (2.7) has a unique disease-free equilibrium point E_3^0 and E_3^0 is globally asymptotically stable; and when $R_0^c > 1$, Model (2.7) has a unique endemic disease equilibrium point E_3^*. If $R_0^c > \max\{2[\beta_E(1-B_c)+\rho_E\beta_E B_c](1-B_c+qB_c)/\mu, 2[\beta_A(1-B_c)+\rho_A\beta_A B_c](1-B_c+qB_c)/\mu, 2\beta_I(1-B_c+qB_c)/\mu\}$, then E_3^* is locally asymptotically stable. Within the model framework, numerical simulations show that behavioral changes significantly inhibit the spread of diseases, and that increasing the return difference $f_c - f_n$ via the parameters (ξ_c, ξ_n, C) leads to more behavioral changes in (S, E, A). Finally, we used COVID-19 data from Romania in two stages to illustrate the model's behavior and discussed the impact of some parameters on diseases. Under the model's assumptions, the following results are obtained. (i) A higher value of the information function may lead to a larger proportion of individuals changing their behavior. Furthermore, according to the model, reducing the decay rate η or the additional cost C, or increasing parameter a, results in an increase in the information function. These are model-based theoretical insights, not empirical prescriptions. (ii) Lower contact rates β_E and β_I or a higher cure rate γ_I leads to a decrease in the number of infections $I(t)$. In summary, from the model's perspective, increasing the information function or reducing contact between susceptible and infected / exposed individuals appears critical to reducing disease transmission.

Use of AI tools declaration

The authors declare they have not used Artificial Intelligence (AI) tools in the creation of this article.

Acknowledgments

This research was funded by the President's Fund Project of Xinjiang University of Political Science and Law (Grant No. XZZK2025018).

Data Availability Statement

The data presented in this study are available upon request from the corresponding author.
We thank reviewers and editors for their constructive and useful advice for improving this paper.

Conflict of interest

The authors declare that they have no conflict of interest.

References

1. T. Ichinomiya, H. Murata, M. Sekino, S. Nakaji, O. Yoshitomi, T. Hara, et al., Tracheobronchial stent insertion under venovenous extracorporeal membrane oxygenation in a patient with coronavirus disease 2019, *J. Cardiothorac. Vasc. Anesth.*, **36** (2022), 2548–2552. https://doi.org/10.1053/j.jvca.2021.09.009
2. H. Abboud, F. Z. Abboud, H. Kharbouch, Y. Arkha, N. El Abbadi, A. El Ouahabi, COVID-19 and SARS-CoV-2 infection: Pathophysiology and clinical effects on the nervous system, *World Neurosurg.*, **140** (2020), 49–53. https://doi.org/10.1016/j.wneu.2020.05.193
3. G. Mark, Natural history of COVID-19 and coronavirus disease, *J. Biomed. Sci.*, **12** (2023), 1–3.
4. S. Ansumali, S. Kaushal, A. Kumar, M. K. Prakash, M. Vidyasagar, Modelling a pandemic with asymptomatic patients, impact of lockdown and herd immunity, with applications to SARS-CoV-2, *Annu. Rev. Control*, **50** (2020), 432–447. https://doi.org/10.1016/j.arcontrol.2020.10.003
5. A. Singh, M. K. Bajpai, SEIHCRD model for COVID-19 spread scenarios, disease predictions and estimates the basic reproduction number, case fatality rate, hospital, and ICU beds requirement, *Comput. Model. Eng. Sci.*, **125** (2020), 991–1031. https://doi.org/10.32604/cmes.2020.012503
6. E. A. Iboi, O. Sharomi, C. N. Ngonghala, A. B. Gumel, Mathematical modeling and analysis of COVID-19 pandemic in nigeria, *Math. Biosci. Eng.*, **17** (2020), 7192–7220. https://doi.org/10.3934/mbe.2020369
7. L. Brugnano, F. Iavernaro, P. Zanzottera, A multiregional extension of the sir model, with application to the COVID-19 spread in italy, *Math. Methods Appl. Sci.*, **44** (2021), 4414–4427. https://doi.org/10.1002/mma.7039
8. A. M. Ramos, M. R. Ferrandez, M. Vela-Pérez, A. B. Kubik, B. Ivorra, A simple but complex enough θ-SIR type model to be used with COVID-19 real data. Application to the case of Italy, *Physica D*, **421** (2021), 132839. https://doi.org/10.1016/j.physd.2020.132839
9. H. Lu, Y. Ding, S. Gong, S. Wang, Mathematical modeling and dynamic analysis of SIQR model with delay for pandemic COVID-19, *Math. Biosci. Eng.*, **18** (2021), 3197–3214. https://doi.org/10.3934/mbe.2021159
10. S. Chatterjee, A. Sarkar, S. Chatterjee, M. Karmakar, R. Paul, Studying the progress of COVID-19 outbreak in india using SIRD model, *Indian J. Phys.*, **95** (2021), 1941–1957. https://doi.org/10.1007/s12648-020-01766-8

11. P. Poletti, B. Caprile, M. Ajelli, A. Pugliese, S. Merler, Spontaneous behavioural changes in response to epidemics, *J. Theor. Biol.*, **260** (2009), 31–40. https://doi.org/10.1016/j.jtbi.2009.04.029
12. P. Poletti, M. Ajelli, S. Merler, Risk perception and effectiveness of uncoordinated behavioral responses in an emerging epidemic, *Math. Biosci.*, **238** (2012), 80–89. https://doi.org/10.1016/j.mbs.2012.04.003
13. S. Funk, M. Salathé, V. A. A. Jansen, Modelling the influence of human behaviour on the spread of infectious diseases: A review, *J. R. Soc. Interface*, **7** (2010), 1247–1256. https://doi.org/10.1098/rsif.2010.0142
14. F. Verelst, L. Willem, P. Beutels, Behavioural change models for infectious disease transmission: a systematic review (2010–2015), *J. R. Soc. Interface*, **13** (2016), 20160820. https://doi.org/10.1098/rsif.2016.0820
15. P. C. Jentsch, M. Anand, C. T. Bauch, Prioritising COVID-19 vaccination in changing social and epidemiological landscapes, *Lancet Infect. Dis.*, **21** (2021), 1097–1106. https://doi.org/10.1016/S1473-3099(21)00057-8
16. F. Saldaña, H. Flores-Arguedas, J. A. Camacho-Gutiérrez, I. Barradas, Modeling the transmission dynamics and the impact of the control interventions for the COVID-19 epidemic outbreak, *Math. Biosci. Eng.*, **17** (2020), 4165–4183. https://doi.org/10.3934/mbe.2020231
17. F. Wang, L. Cao, X. Song, Mathematical modeling of mutated COVID-19 transmission with quarantine, isolation and vaccination, *Math. Biosci. Eng.*, **19** (2022), 8035–8056. https://doi.org/10.3934/mbe.2022376
18. Q. Cui, Z. Hu, Y. Li, J. Han, Z. Teng, J. Qian, Dynamic variations of the COVID-19 disease at different quarantine strategies in Wuhan and mainland China, *J. Infect. Public Health*, **13** (2020), 849–855. https://doi.org/10.1016/j.jiph.2020.05.014
19. M. Mandal, S. Jana, S. K. Nandi, A. Khatua, S. Adak, T. K. Kar, A model-based study on the dynamics of COVID-19: Prediction and control, *Chaos Solitons Fractals*, **136** (2020), 109889. https://doi.org/10.1016/j.chaos.2020.109889
20. R. Zhang, B. Xie, Y. Kang, M. Liu, Modeling and analyzing quarantine strategies of epidemic on two-layer networks: Game theory approach, *J. Biol. Syst.*, **31** (2023), 21–35. https://doi.org/10.1142/S021833902350002X
21. S. K. Biswas, N. U. Ahmed, Mathematical modeling and optimal intervention strategies of the COVID-19 outbreak, *Quant. Biol.*, **9** (2021), 84–92. https://doi.org/10.15302/J-QB-020-0229
22. A. Das, A. Dhar, S. Goyal, A. Kundu, S. Pandey, COVID-19: Analytic results for a modified SEIR model and comparison of different intervention strategies, *Chaos Solitons Fractals*, **144** (2021), 110595. https://doi.org/10.1016/j.chaos.2020.110595
23. S. W. Teklu, Mathematical analysis of the transmission dynamics of COVID-19 infection in the presence of intervention strategies, *J. Biol. Dyn.*, **16** (2022), 640–664. https://doi.org/10.1080/17513758.2022.2111469

24. F. Arif, Z. Majeed, J. Ul Rahman, N. Iqbal, J. Kafle, Mathematical modeling and numerical simulation for the outbreak of COVID-19 involving loss of immunity and quarantined class, *Comput. Math. Methods Med.*, **2022** (2022), 3816492. https://doi.org/10.1155/2022/3816492
25. B. Tang, W. Zhou, X. Wang, H. Wu, Y. Xiao, Controlling multiple COVID-19 epidemic waves: An insight from a multi-scale model linking the behavior change dynamics to the disease transmission dynamics, *Bull. Math. Biol.*, **84** (2022), 106. https://doi.org/10.1007/s11538-022-01061-z
26. S. Funk, M. Salathé, V. A. A. Jansen, Modelling the influence of human behaviour on the spread of infectious diseases: A review, *J. R. Soc. Interface*, **7** (2010), 1247–1256. https://doi.org/10.1098/rsif.2010.0142
27. P. C. Jentsch, M. Anand, C. T. Bauch, Prioritising COVID-19 vaccination in changing social and epidemiological landscapes, *Lancet Infect. Dis.*, **21** (2021), 1097–1106. https://doi.org/10.1016/S1473-3099(21)00057-8
28. P. Manfredi, A. D'Onofrio, *Modeling the Interplay Between Human Behavior and the Spread of Infectious Diseases*, Springer, 2013. https://doi.org/10.1007/978-1-4614-5474-8_6
29. F. Verels, L. Willem, P. Beutel, Behavioural change models for infectious disease transmission: A systematic review (2010–2015), *J. R. Soc. Interface*, **13** (2016), 20160820. https://doi.org/10.1098/rsif.2016.0820
30. Q. Yuan, J. Zhang, Z. Wang, H. Wang, Optimal control of SISV infectious disease model based on information nonlinear intervention (in Chinese), *Nat. Sci. J. Hainan Univ.*, **41** (2023), 1–10. https://doi.org/10.15886/j.cnki.hdxbzkb.2023.0001
31. J. Zhang, H. Wang, Stability analysis and optimal control of HBV infectious disease model under information intervention (in Chinese), *Nat. Sci. J. Hainan Univ.*, **40** (2022), 39–49. https://doi.org/10.15886/j.cnki.hdxbzkb.2022.0005
32. Y. Iwamura, J. Tanimoto, E. Fukuda, Effect of intermediate defense measures in voluntary vaccination games, *J. Stat. Mech.: Theory Exp.*, **2016** (2016), 093501. https://doi.org/10.1088/1742-5468/2016/09/093501
33. Y. Lu, A. D. Miguel-Arribas, L. Shi, Influence of social peers on vaccine hesitancy under imperfect vaccination, *Appl. Math. Comput.*, **491** (2025), 129214. https://doi.org/10.1016/j.amc.2024.129214
34. I. Nishimura, M. R. Arefin, Y. Tatsukawa, S. Utsumi, M. A. Hossain, J. Tanimoto, Social dilemma analysis on vaccination game accounting for the effect of immunity waning, *Chaos Solitons Fractals*, **171** (2023), 113426. https://doi.org/10.1016/j.chaos.2023.113426
35. P. van den Driessche, J. Watmough, Reproduction numbers and subthreshold endemic equilibria for compartmental models of disease transmission, *Math. Biosci.*, **180** (2002), 29–48. https://doi.org/10.1016/S0025-5564(02)00108-6

AIMS Press